Remanence enhancement based on $L1_0$ ordering in Fe–Pt permanent magnets

Y. Tanaka[a] and K. Hisatsune
Department of Dental Materials Science, Nagasaki University School of Dentistry, Nagasaki 852-8588, Japan

(Received 18 June 2002; accepted 3 January 2003)

This study investigated the relationship between the hard magnetic properties and microstructure of bulk FePt magnets, which can potentially be used in dental prostheses. A high level of remanence was obtained in a Fe–39.5 mol %Pt alloy aged at 873 K, in which minute FePt ordered domains of about 10 nm in size were uniformly created. The change in the maximum energy product of this alloy was in good agreement with the level of remanence: they both decreased with increasing aging time, and the size of the ordered domains gradually grew. The remanence ratio of as-quenched Fe–40 mol %Pt magnet has been estimated at 0.69, despite the morphological isotropy of the magnet. Remanence enhancement occurred in an FePt single phase without the presence of the magnetically soft disordered phase, since the spring back phenomenon was not observed in the recoil curve measurements, and the entire area was covered with minute FePt ordered domains. The hard magnetic properties were enhanced at the optimum ordered domain size of about 10 nm. This study found that the ordered domains behaved as a single magnetic domain particle and improved remanence through intergranular exchange interaction. © *2003 American Institute of Physics.* [DOI: 10.1063/1.1555675]

I. INTRODUCTION

The $L1_0$-type ordered phase in Fe–Pt alloys has been reported to have high magnetic crystalline anisotropy ($K=7$ MJ m^{-3}) in the *c*-axis direction.[1] Recently, Fe–Pt thin films were employed in applications such as perpendicular magnetization films,[2] hard magnetic films producing 500 kJ m^{-3} of energy,[3] and magnetic recording media at areal densities in the range of terabits/in.^{2}.[4] In addition, it is possible to use these alloys as biomaterials in medicine and dentistry, since Fe–Pt alloys possess excellent corrosion resistance[5] due to the high platinum content. They may be applied to dentistry as castable magnetic attachments to retain prostheses in the oral cavity.[6,7] The composition of the optimum hard magnetic properties in the bulk system differs from that in the thin film system.[8] As shown in the Fe–Pt phase diagram[9] (Fig. 1), the hardest magnetic performance of all the metallic systems (with the exception of rare-earth-based magnets) can be obtained[10,11] in a region near the 40 mol %Pt composition. The magnetic properties are very sensitive to the alloy composition, the heat treatment conditions, etc. since Fe–Pt alloys show excellent magnetic performance in the iron-rich nonstoichiometric compositional range of the Fe–Pt ordered phase region.

Previously, we used transmission electron microscopy (TEM) to investigate the relationship between magnetic properties and the degree of ordering created by aging an Fe–39.5 mol %Pt alloy at a elevated temperature.[12] The maximum coercivity (277 kA/m) was obtained in our study after aging the Fe–39.5 mol %Pt alloy at 873 K for 36 s. The dark field TEM image using a 001 superlattice reflection for the alloy possessing excellent coercivity revealed that the entire area of the alloy was covered with minute ordered domains aligned in the ⟨110⟩ direction, and that the alloy was in ordered single phase. When the twin structure of the tetragonal ordered phase ($L1_0$-type cell) formed, the coercivity decreased, suggesting that high coercivity might be the result of the minute ordered domains playing the role of a single magnetic domain particle. On the other hand, the highest maximum energy product was obtained under a different aging condition from that used to find the highest coercive force. Because the maximum energy product relates to the total performance of a Fe–Pt magnet, it is important to clarify the origin of the change in the maximum energy product.

The purpose of this study was to examine in detail the relationship between the microstructure and the magnetic properties of the Fe–Pt alloy magnet using a vibrating sample magnetometer (VSM) and TEM.

II. EXPERIMENTAL PROCEDURE

Sample alloys were melted using a high-frequency furnace in a sintered alumina crucible under argon atmosphere, and the melt was drawn into a silica tube (3 mm ID) to produce an alloy rod. The sample then became an isotropic magnet without morphological anisotropy. After vacuum sealing the silica tube, the sample alloy underwent solution treatment at 1598 K for 2.7 ks, and was quenched in ice water. The sample was subsequently subjected to heat treatment at 873 K. Measurement of the magnetic properties was carried out using a vibrating sample magnetometer (VSM, Tamakawa TM-VSM2430HGC) under a maximum external magnetic field of 1.6 or 2.4 MA m^{-1}. The calibration and

[a]Electronic mail: y-tanaka@net.nagasaki-u.ac.jp

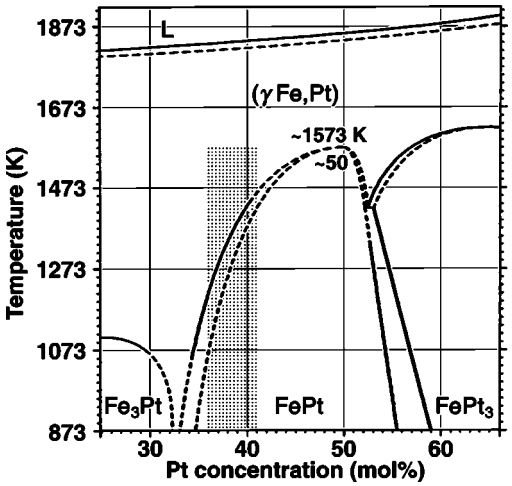

FIG. 1. Part of the Fe–Pt alloy phase diagram (see Ref. 9). Hard magnetic properties are obtained in the shaded compositional range (see Ref. 10).

demagnetizing field compensation of the magnetization process were carried out using a Ni standard sample that was isomorphic with the measured sample. One fresh sample was used to obtain magnetic data for one heat treatment period. Each sample was then subjected to TEM observation (JEOL JEM-2010 HT and Philips CM 12 electron microscopes). The TEM observation sample, which was sliced from the VSM sample, was thinned using electropolishing with concentrated hydrochloric acid[13] or a liquid mixture of sulfuric acid and phosphoric acid.[14]

III. RESULTS AND DISCUSSION

Figure 2(a) shows the changes of coercivity (H_c) and the maximum energy product [$(BH)_{max}$] in the Fe–39.5 mol %Pt alloy after heat treatment at 873 K, which were reported previously by Tanaka *et al.*[12] It can be seen that the changes do not correspond to each other. Although the largest coercive force (277 kA m^{-1}) is obtained using a heat treatment of 36 ks, the maximum energy product decreases during this amount of time (36 ks). Changes in the residual magnetization (I_r) and the magnetization after applying an external magnetic field of 1.6 MA m^{-1} (20 kOe) (I_{20}) are shown in Fig. 2(b). The changes in the maximum energy product and the residual magnetization resemble each other. In fact, the residual magnetization seems to influence the change in the maximum energy product. Figure 2(c) shows the change in residual magnetization normalized by I_{20}. Although this I_r/I_{20} value is not the remanence ratio itself, which is the normalized residual magnetization divided by the saturation magnetization, it is possible to regard I_r/I_{20} as an indicator of the remanence of the Fe–Pt magnet. A high level of remanence is obtained under the conditions used to achieve a high energy product. During preparation, the sample becomes an isotropic magnet without morphological anisotropy, and therefore, the crystal grain has a random orientation. The magnetic anisotropy of the FePt magnet is in the uniaxial *c*-axis direction.[1] In the case of a morphologically isotropic magnet made of crystals with strong easy-axis anisotropy, the remanence field is expected to be ~1/2 of the saturated field.[15]

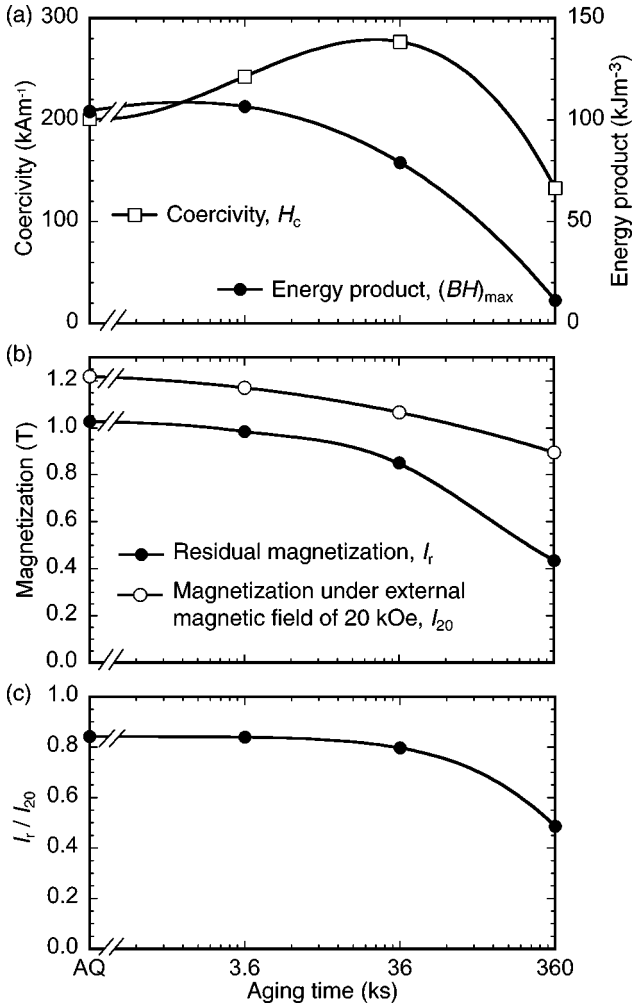

FIG. 2. Magnetic properties of the Fe–39.5 mol %Pt alloy aged at 873 K: (a) coercivity (H_c) and energy product [$(BH)_{max}$] obtained previously (see Ref. 12); (b) residual magnetization (I_r) and magnetization (I_{20}) using the external magnetic field of 1.6 MA m^{-1} (20 kOe); (c) the ratio of I_r /I_{20}.

High remanence was revealed in the present FePt magnet, and a phenomenon similar to remanence enhancement[16] seen in nanocomposite magnets[16] and exchange spring magnets[17] may be occurring. The vector sum of the magnetization will increase if there is ferromagnetic exchange interaction between crystal grains. It is probable that this effect becomes important in nanosize crystal grains because the areal ratio of the interface to the volume increases. Therefore, the residual magnetization may be improved by the intergranular exchange interaction in the vicinity of the interface and the grain boundary. In addition, a nanocomposite magnet can be produced in cases where the soft magnetic phase is intermingled with the hard magnetic phase when the crystal grain size is fine (about 10 nm). In this situation, the direction of the magnetic moment in the soft phase easily rotates in order to become parallel.[18]

A previous study showed by means of dark field TEM observation using superlattice reflection that ordered domains of about 10 nm are formed in the FePt magnet, giving

it excellent magnetic properties.[12] Since the *c* axis of the FePt ordered phase can take any of the *x*, *y*, and *z* directions of the parent disordered fcc phase, three orientational variants exist for the ordered domain. However, only one orientational variant is visible when the FePt ordered phase is observed by TEM. In the [001] zone axis incident beam condition, the superlattice reflections of the three orientational variants (001_x, 001_y, and 110_z) appeared in the diffraction plane at the same time. Each dark field TEM image illuminated the ordered domains of a particular orientational variant. Three negative films of the TEM micrographs were captured and digitized (Apple Power Macintosh 8500/120 computer and Apple Color OneScanner 1200/30 with a transparent manuscript unit). A dark field image, in which all orientational variants were combined, is displayed in one micrograph (Fig. 3).

In the as-quenched sample, ordered domains almost 10 nm in size were produced in the entire area during quenching after the solution heat treatment. The size of the ordered domains gradually grew with increasing aging time at 873 K. As seen in Fig. 2(c), coarsening of the ordered domain was in good agreement with the decrease of remanence. It is speculated that the remanence may have been improved by the effect of the interface as well by as the nanocomposite magnet, since the decrease in the ratio of the interface to the volume with the gradual growth of the 10-nm ordered domain led to degradation of the remanence.

In addition, magnetic measurement was carried out under the maximum external magnetic field of 2.4 MA m^{-1} (30 kOe). The hysteresis loops of the as-quenched Fe–40 mol %Pt and Fe–38 mol %Pt alloys are shown in Fig. 4(a). The Fe–40 mol %Pt and Fe–38 mol %Pt alloys show hard and soft-magnetic behavior, respectively. Values for the coercive force, the residual magnetization, and the maximum energy product in the Fe–40 mol %Pt magnet were 211 kA m^{-1}, 1.0 T, and 93 kJ m^{-3}, respectively. However, the magnetization of the Fe–40 mol %Pt magnet was not saturated even in the external magnetic field of 2.4 MA m^{m-1}. On the other hand, the magnetization of the soft magnetic Fe–38 mol %Pt alloy was saturated by the external magnetic field of 2.4 MA m^{-1}, and saturation magnetization of 1.45 T was obtained. If the saturation magnetization of the Fe–40 mol %Pt magnet is also assumed to be comparable to the Fe–38 mol %Pt alloy, the remanence ratio can be estimated as 0.69. The remanence enhancement is confirmed, although the remanence ratio is lower than the value reported for nanocomposite magnets.[16]

The spring back phenomenon is well known in the minor loop measurement of nanocomposite magnets. The recoil permeability for regular permanent magnets is very low, since it consists of the hard magnetic phase with low reversible permeability. On the other hand, the recoil curve for the nanocomposite magnets yields high permeability because of the presence of the soft magnetic phase. Figure 4(b) shows an example of the as-quenched Fe–40 mol %Pt alloy. The recovery of magnetization is quite low, and the spring back phenomenon is not observed. The behavior of the recoil curve for the as-quenched Fe–40 mol %Pt alloy is similar to that for a regular permanent magnet, which indicates that the soft magnetic phase does not exist in the as-quenched Fe–40 mol %Pt alloy. Our previous study[12] concluded that the highest coercivity was achieved with the single phase condition of the FePt ordered phase, and the present study of minor loop measurement lends support to that conclusion.

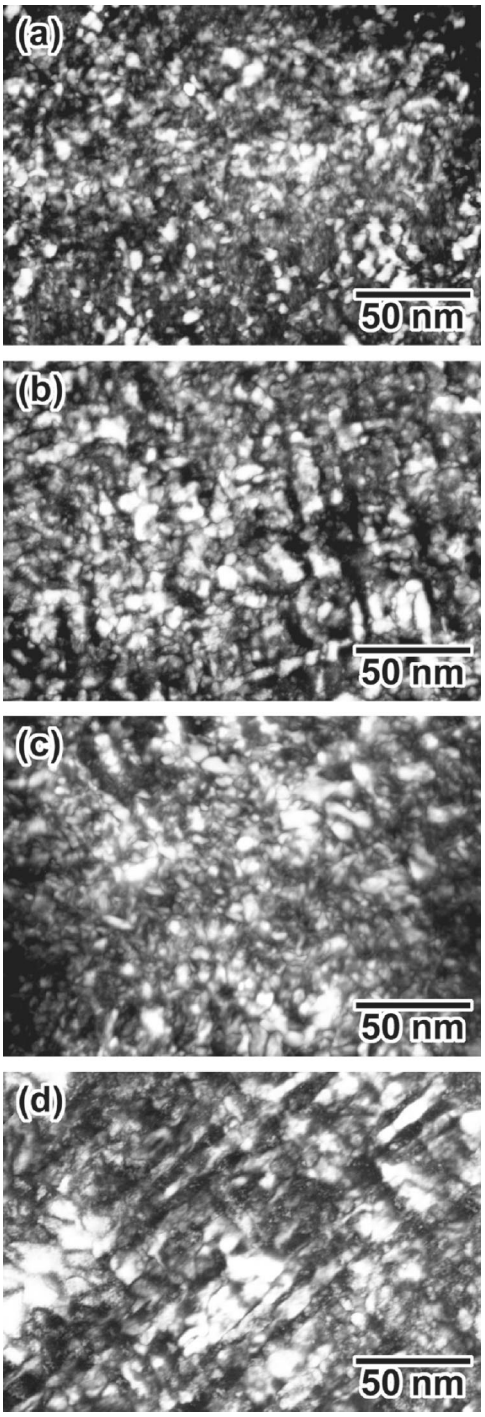

FIG. 3. Images of the Fe–39.5 mol %Pt alloy from 001_x, 001_y, and 110_z dark field TEM images: (a) as-quenched; (b) aged at 873 K for 3.6 ks; (c) 873 K for 36 ks; (d) 873 K for 360 ks.

A high-resolution electron micrograph of the as-quenched Fe–40 mol %Pt alloy from the [001] zone axis direction is shown in Fig. 5. All reflections up to the 220 spot were selected for imaging. The horizontal and vertical directions are the ⟨110⟩ direction. The *c*-axis direction of the

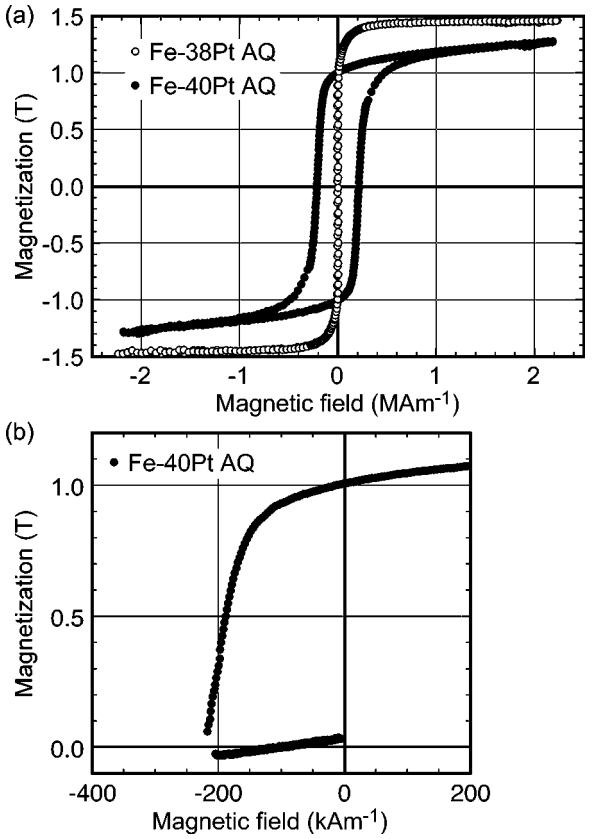

FIG. 4. (a) Hysteresis loops of the as-quenched Fe–40 mol %Pt and Fe–38 mol %Pt alloys; (b) recoil curve of the as-quenched Fe–40 mol %Pt alloy.

FePt ordered phase is seen parallel (arrows) and perpendicular (circle) to the foil specimen. Each ordered domain, with *x*- and *y*-orientational variants shown by the arrows, and *z*-orientational variant shown by the circle, is about 10 nm. It can be seen that the entire area is covered with the ordered domains. The disordered fcc phase is not found between the ordered domains. If the disordered fcc phase existed, it would behave as a soft magnetic phase. However, the spring back phenomenon did not appear in the minor loop measurement, and existence of the disordered phase could not be confirmed even with high- resolution TEM. The thickness of the magnetic domain wall in the FePt magnet must be very small because the crystal magnetic anisotropy of the FePt ordered phase is very high ($K=7$ MJ m^{-3}).[1] Zhang and Soffa have estimated the thickness to be 4 nm.[19] Since the ordered domain size of about 10 nm is slightly larger than the magnetic domain wall thickness, it is anticipated that each ordered domain will behave as a single magnetic domain particle. Such a single magnetic domain particle pins the motion of the magnetic domain wall. As a result, the present alloy could acquire high coercivity. When the ordered domain size is small enough, the ratio of the interface between the ordered variants to the volume increases. Therefore, the remanence seems to be enhanced because the contribution of the intergranular exchange interaction to the magnetization increases. However, if the ordered domain size were as small as the thickness of a magnetic domain wall, it would not be possible for the domains to work as a single domain particle.

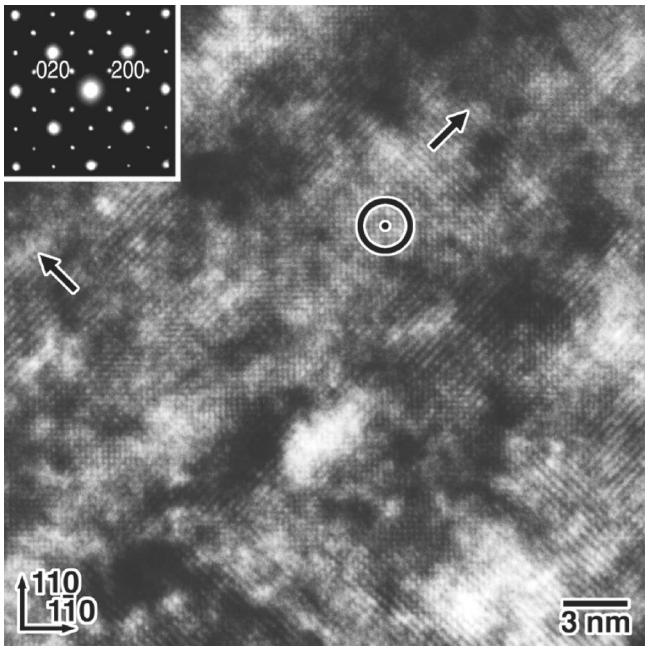

FIG. 5. High-resolution electron micrograph of the as-quenched Fe–40 mol %Pt alloy. The arrows and circle indicate the directions of the *c* axis of the FePt ordered phase parallel with and perpendicular to the foil specimen, respectively.

In short, the optimum ordered domain size should not be so small that it acts as a single magnetic domain particle, nor should it be too large to contribute to the intergranular exchange interaction. The ordered domain size of about 10 nm seems to be the optimum size, and thus, the as-quenched Fe–40 mol %Pt alloy exhibits high magnetic performance because of its maximum energy product.

IV. CONCLUSIONS

(1) Remanence enhancement was observed when hard magnetic performance was obtained in an FePt magnet with an ordered phase.

(2) The remanence ratio of the Fe–39.5 mol %Pt alloy aged at 873 K decreased with a gradual increase in the ordered domain size of about 10 nm.

(3) Remanence enhancement was observed in the single phase of FePt ordered domains when the soft magnetic phase was not present.

(4) The optimum ordered domain size in the FePt magnet seemed to be about 10 nm. The size is critical: it must be sufficiently large to work as a single magnetic domain particle but small enough to improve the remanence through intergranular exchange interaction.

ACKNOWLEDGMENTS

The authors wish to thank Dr. N. Kimura of Honda R&D and Dr. K. Hono of the National Research Institute for Metals for sample preparation and useful discussions and Professor H. Fukunaga of Nagasaki University for useful discussions on remanence enhancement. A part of this study was performed under the Visiting Research Program of the Institute for Material Research, Tohoku University. Partial finan-

cial support for this work was provided by a Grant-in-Aid for the Encouragement of Young Scientists from the Japanese Ministry of Education, Science, Sports and Culture.

[1] O. A. Ivanov, L. V. Solina, V. A. Demshina, and L. M. Msgat, Phys. Met. Metallogr. **35**, 81 (1973).
[2] M. Watanabe and M. Homma, Jpn. J. Appl. Phys., Part 1 **35**, 1264 (1996).
[3] J. P. Liu, C. P. Luo, Y. Liu, and D. J. Sellmyer, Appl. Phys. Lett. **72**, 483 (1998).
[4] S. Sun, C. B. Murray, D. Weller, L. Folks, and A. Moser, Science **287**, 1989 (2000).
[5] O. Okuno, F. T. Iimuro, T. Nakano, H. Hamanaka, Y. Kinouchi, and Y. Matsui, J. J. Mag. Dent. **1**, 14 (1992) (in Japanese).
[6] T. Kanno, M. Yoda, K. Kimura, Y. Takada, K. Iijima, O. Okuno and T. Nakayama, J. J. Mag. Dent. **5**, 58 (1996) (in Japanese).
[7] T. Nakayama, M. Watanabe, M. Homma, T. Kanno, K. Kimura, and O. Okuno, J. Magn. Soc. Jpn. **21**, 377 (1997) (in Japanese).
[8] M. H. Hong, K. Hono, and M. Watanabe, J. Appl. Phys. **84**, 4403 (1998).
[9] H. Okamoto, *Binary Alloy Phase Diagrams, 2nd ed., edited by T. B. Massalski (ASM, Metals Park, OH, 1990), Vol. 2, p. 1752.*
[10] K. Watanabe and H. Masumoto, Trans. JIM **26**, 362 (1985).
[11] K. Watanabe, Trans. JIM **32**, 292 (1990).
[12] Y. Tanaka, N. Kimura, K. Hono, K. Yasuda, and T. Sakurai, J. Magn. Magn. Mater. **170**, 289 (1997).
[13] B. Zhang and W. A. Soffa, Phys. Status Solidi A **131**, 707 (1992).
[14] T. Tadaki and K. Shimizu, Trans. JIM **11**, 44 (1970).
[15] E. C. Stoner and E. P. Wohlfarth, Philos. Trans. R. Soc. London, Ser. A **240**, 599 (1948).
[16] R. Coehoorn, D. B. de Mooij, and C. de Waard, J. Magn. Magn. Mater. **80**, 101 (1989).
[17] E. F. Kneller and R. Hawig, IEEE Trans. Magn. **27**, 3588 (1991).
[18] H. Fukunaga and H. Inoue, Jpn. J. Appl. Phys., Part 1 **31**, 1347 (1992).
[19] B. Zhang and W. A. Soffa, Scr. Metall. Mater. **30**, 683 (1994).